The RalA GTPase Is a Central Regulator of Insulin Exocytosis from Pancreatic Islet Beta Cells*

Jamie A. Lopez[‡1,2], **Edwin P. Kwan**[§1,3], **Li Xie**[§1], **Yu He**[§], **David E. James**[‡4], and **Herbert Y. Gaisano**[§5]

From the ‡Diabetes and Obesity Program, Garvan Institute of Medical Research, Sydney, New-South Wales, Australia 2010 and the §Department of Physiology and Medicine, University of Toronto, Toronto, Ontario, Canada M5S 1A8

RalA is a small GTPase that is thought to facilitate exocytosis through its direct interaction with the mammalian exocyst complex. In this study, we report an essential role for RalA in regulated insulin secretion from pancreatic beta cells. We employed lentiviral-mediated delivery of RalA short hairpin RNAs to deplete endogenous RalA protein in mouse pancreatic islets and INS-1 beta cells. Perifusion of mouse islets depleted of RalA protein exhibited inhibition of both first and second phases of glucose-stimulated insulin secretion. Consistently, INS-1 cells depleted of RalA caused a severe inhibition of depolarization-induced insulin exocytosis determined by membrane capacitance, including a reduction in the size of the ready-releasable pool of insulin granules and a reduction in the subsequent mobilization and exocytosis of the reserve pool of granules. Collectively, these data suggest that RalA is a critical component in biphasic insulin release from pancreatic beta cells.

Ral proteins, of which there are two isoforms, RalA and RalB, are members of the Ras small GTPase superfamily (1) and have been implicated in multiple cellular events including endocytosis (2), filopodia formation (3), and oncogenic transformation (4). Ral proteins have also emerged as important regulators of exocytosis. Ral has previously been reported to regulate the trafficking of proteins to the basolateral membrane in polarized epithelial cells and the secretion of human growth hormone and norepinephrine from neuroendocrine cells (5, 6).

Postprandial insulin secretion from beta cells within the pancreatic islets of Langerhans regulates blood glucose homeostasis by facilitating the uptake of glucose from the bloodstream into insulin-responsive tissues (7). Insulin is stored inside large dense core granules within the beta cell and undergoes exocytosis in a biphasic pattern in response to elevated glucose concentrations. It has been suggested that spatially separable insulin granule populations account for the biphasic nature of insulin secretion, with the primed predocked or readily releasable pool (RRP)[6] thought to contribute to the first phase of insulin secretion, whereas the second phase of insulin secretion is thought to require recruitment of the reserve pool of granules (8).

RalA is believed to exert its functional effects by binding to its effector proteins. Its most notable effector is the mammalian exocyst complex. The exocyst complex has been postulated to regulate secretory vesicle tethering at the plasma membrane, and RalA has been found to bind the exocyst complex in a GTP-specific manner (5, 9). The role of RalA/exocyst in vesicle tethering is believed to be a critical event in the exocytic process that precedes granule priming and exocytotic fusion. Interestingly, a recent study by Tsuboi *et al.* (10) demonstrated that the exocyst complex is required for insulin granule docking in MIN6 beta cells. Overexpression of truncated forms of three exocyst subunits, Sec6, Sec8, and Sec10, inhibited glucose- and KCl-induced insulin secretion, which on evanescent (total internal reflection fluorescence) microscopy was attributed to a reduction in the number of docked insulin granules at the plasma membrane.

In the present study, we have investigated the role of RalA in insulin secretion. RalA protein depletion in mouse pancreatic islets and insulinoma cell lines inhibited biphasic insulin release, which could be attributed to a reduction of the RRP of insulin granules and further reduction in the subsequent mobilization of the reserve pool of granules. Adenoviral overexpression of RalA*wt* and its nucleotide mutants in MIN6 cells showed that the function of RalA in secretagogue-stimulated insulin secretion is in part mediated via guanine nucleotide signaling. We propose that RalA plays a positive role in regulating the entry of granules into the readily releasable pool.

EXPERIMENTAL PROCEDURES

Materials—The following antibodies were used: mouse anti-Myc antibodies (clone 9E10) (Roche Applied Science, Basel, Switzerland), rabbit anti-Myc antibodies (AbCam, Cambridge, UK), mouse anti-β-actin and mouse anti-insulin antibodies (I2018) (Sigma-Aldrich), anti-mouse infrared dye-conjugated

[6] The abbreviations used are: RRP, readily releasable pool; Cm, cell membrane capacitance; shRNA, short hairpin RNA; GFP, green fluorescent protein; GST, glutathione *S*-transferase; PBS, phosphate-buffered saline; KRB, Krebs-Ringer bicarbonate; GTPγS, guanosine 5′-3-*O*-(thio)triphosphate; KD, knockdown.

secondary antibodies (Rockland Immunochemicals); anti-mouse and anti-rabbit Alexa Fluor-488-conjugated antibodies (Molecular Probes, Leiden, The Netherlands); and anti-mouse Cy3-conjugated antibodies (Jackson ImmunoResearch, Westgrove, PA). Antibodies against Sec6 were obtained from C. Yeaman (University of Iowa, Iowa City, IA). The RalA shRNA (pU6.GK) pBluescript construct was obtained from M. Graham (Benitec Ltd.). The RalA shRNA was designed on the target sequence (5′-ggcaggtttctgtagaaga-3′). The Htr-1 and RalA shRNA cassettes were subcloned into the pHIV7-GFP lentiviral expression vector. The pHIV7-GFP lentiviral expression vector and packaging vectors pCgp (gag/pol vector), pCMV-rev2 (rev vector), and pCMV-G (VSV-G vector) were obtained from J. Rossi (Beckman Research Institute of the City of Hope, Duarte, CA). The mycRalA*wt*-pAd, mycRalAG23V-pAd, and mycRalAS28N-pAd adenoviral backbone vectors were generated by PCR amplification of the rat RalA cDNA (obtained from P. Robinson at the Children's Medical Research Institute, Sydney, Australia), and a single Myc epitope was introduced at the N terminus of RalA. The RalA PCR products were subcloned into the pDONR201 entry vector (Invitrogen) using BP recombination (Invitrogen). The G23V and S28N mutations were introduced using the QuikChange II XL site-directed mutagenesis kit (Stratagene), according to the manufacturer's instructions. This generated three RalA entry clone vectors: mycRalA*wt*-pDONR201, mycRalAG23V-pDONR201, and mycRalAS28N-pDONR201. The RalA entry clone vectors were used in LR recombination reactions (Invitrogen) with the Gateway® adenoviral backbone vector pAd/CMV/V5-DEST (Invitrogen).

Cell Culture—MIN6 cells were cultured in Dulbecco's modified Eagle's medium (Invitrogen) containing 25 mM glucose, 10 mM HEPES, 10% (v/v) fetal calf serum and penicillin/streptomycin at 37 °C/5% CO_2. Prior to insulin secretion experiments, MIN6 cells were cultured in Dulbecco's modified Eagle's medium low glucose medium (containing 6 mM glucose).

GST-RalA Pulldown Experiments—The GST-RalA pulldown experiments were performed as described previously (11), using MIN6 total cell lysates.

Lentivirus Production—HEK293FT cells were seeded into T150 flasks coated with 0.2% (w/v) gelatin in PBS. Cells were transfected at 70–90% confluency using a calcium phosphate-DNA suspension method (12). Each T150 flask was transfected with 29 μg of pDEST/pHIV7.U6.shRNA.CMV-GFP expression vector, 29 μg of pCgp (gag/pol) vector, 9.6 μg of pCMV-rev (rev) vector, and 9.6 μg of pCMV-G (VSV-G) vector in 20 ml of culture medium. At 5–6 h after transfection, the medium was replaced with 12 ml of culture medium containing 6 mM butyric acid. Lentivirus was harvested at 24 h after transfection and replaced with an additional 12 ml of culture medium containing 6 mM butyric acid. The medium was collected from each T150 flask and centrifuged at 1620 × g for 10 min to pellet any cells. The supernatant was transferred to 15 ml, 100,000 molecular weight cutoff, Amicon Ultracel concentration tubes (Amicon Plastics) and centrifuged at 3500 × g for 10–15 min to concentrate the virus medium. At 48 h after transfection, this concentration process was repeated.

Lentivirus Transductions—INS-1 832/13 cells were transduced with concentrated control (Htr-1) or RalA shRNA lentivirus, and stable cell lines were established based on the selection of GFP-positive cells by flow cytometry (BD Biosciences) after 20 passages. Islets were transduced with RalA shRNA or control (Htr-1) shRNA lentivirus at approximate multiplicity of infection of 100 (assuming 3000 cells/islet) for 48 h. Entry of viral particles after transduction was determined by GFP expression observed by epifluorescence imaging on a Nikon TE2000U inverted microscope.

Recombinant Adenovirus Production and Purification—The empty virus control (empty pShuttle virus) was provided by W. Hughes (Garvan Institute, Sydney, Australia). Recombinant RalA adenoviruses were prepared using the Gateway® pAd system (Invitrogen). Each RalA adenovirus was plaque-purified and amplified. Viral titers were determined using the Adeno-X™ rapid titer kit (Clontech Laboratories Inc.).

Adenoviral Transductions, Immunoblotting, and Confocal Microscopy—Twenty-four-well plates were seeded with MIN6 cells 1 day prior to the adenoviral transductions at a density of 3×10^5 cells/well in MIN6 culture medium containing low glucose (6 mM glucose). The following day, each well contained ~3.25×10^5 cells/well. Cells were washed once with 1-ml volumes of MIN6 low glucose culture medium, and this was replaced with 0.5-ml volumes of low glucose medium containing 50 viral particles/cell (multiplicity of infection of 50) of empty virus or RalA viruses followed by incubation at 37 °C/5% CO_2 for 16–20 h. The following day, cells were washed with 1-ml volumes of MIN6 low glucose culture medium and incubated at 37 °C/5% CO_2. At 48 h after transduction, cells were processed for immunoblotting, immunofluorescence microscopy, or insulin secretion assays. For immunoblotting, MIN6 cells were transferred to ice and washed three times with cold PBS. Cells from each well were resuspended in 100 μl of 2% (v/v) SDS in PBS containing Complete protease inhibitor (Roche Applied Science) and lysed by passage through a 22-gauge needle 10 times and twice through a 27-gauge needle. Lysates were heated at 100 °C for 10 min and centrifuged at 16,200 × g for 10 min. The supernatants were retained and analyzed by SDS-PAGE and immunoblotting using anti-RalA, anti-Myc, or anti-β-actin antibodies. For immunofluorescence microscopy, cells were seeded on glass coverslips within 24-well plates. At 48 h after transduction, cells were washed three times in cold PBS, fixed with 3% (v/v) paraformaldehyde in PBS, blocked in 2% (w/v) bovine serum albumin containing 0.1% (w/v) saponin in PBS, and labeled with rabbit or mouse anti-Myc antibodies at 1:200 dilutions and rabbit anti-insulin antibodies at a 1:100 dilution. Cells were subsequently labeled with anti-mouse Alexa Fluor-488, anti-rabbit Alexa Fluor-488, anti-mouse Cy3, or anti-rabbit Cy3 antibodies at 1:200 dilutions. Coverslips were mounted onto glass coverslides using Immuno-Fluore mounting medium (ICN Biomedicals Inc.). The slides were examined using a Leica laser scanning confocal microscope (Leica Microsystems, Wetzlar, Germany). Alexa Fluor-488 and Cy3 fluorophores were excited with the appropriate excitation wavelength. Image processing was carried out using Leica confocal software.

Insulin Secretion Assays—Adenoviral transduced MIN6 cells grown in 24-well plates in MIN6 low glucose culture medium were washed once with Krebs-Ringer bicarbonate (KRB) buffer containing 5 mM $NaHCO_3$, 10 mM HEPES, pH 7.4, 1 mM $CaCl_2$, 0.5% (w/v) bovine serum albumin, 2.8 mM glucose and incubated for an additional 30 min in 0.5 ml of KRB buffer. The buffer was removed, and cells were incubated for 1 h in 0.5 ml of KRB buffer containing each of the secretagogues: KCl (30 mM), glucose/carbachol (25 mM/100 μM), or glucose/KCl (25 mM/30 mM). After 1 h, cells were transferred to ice, and fractions were collected from each well. The amounts of secreted insulin were determined using a rat insulin radioimmunoassay kit (Linco Research, Inc.) according to the manufacturer's instructions.

Patch Clamp Membrane Capacitance Measurements—Patch electrodes were pulled from 1.5-mm thin-walled borosilicate glass, coated close to the tip with orthodontic wax (Butler, Guelph, Ontario, Canada), and polished to a tip resistance of 2–4 megaohms when filled with intracellular solution. The intracellular solution contained: 125 mM potassium glutamate, 10 mM KCl, 10 mM NaCl, 1 mM $MgCl_2$, 5 mM HEPES, 0.05 mM EGTA, 3 mM MgATP, 0.1 mM cAMP; pH to 7.1. The extracellular solution consisted of 138 mM NaCl, 5.6 mM KCl, 1.2 mM $MgCl_2$, 2.6 mM $CaCl_2$, 5 mM HEPES, and 5 mM D-glucose; pH to 7.4. Cell membrane capacitance (Cm) was estimated by the Lindau-Neher technique (13), implementing the "Sine + DC" feature of the Lock-in module (40 mV peak-to-peak and a frequency of 500 Hz) in the whole-cell configuration. Recordings were conducted using an EPC10 patch clamp amplifier and the Pulse and X-Chart software programs (HEKA Electronik, Lambrecht, Germany). Exocytic events were elicited by a train of eight 500-ms depolarization pulses (1-Hz stimulation frequency) from −70 to 0 mV. All recordings were performed at 30 °C.

Islet Isolation—Islets were isolated from male C57B6/J mice (22–25 g of body weight) (Charles River Laboratories Inc.). Two milliliters of 2 mg/ml collagenase (Sigma) was injected into the common bile duct for pancreatic digestion, as described previously (14). Isolated islets were cultured in suspension culture in RPMI 1640 supplemented with 11 mM D-glucose, 10% fetal bovine serum, 100 units/ml penicillin, and 100 μg/ml streptomycin at 37 °C with 5% CO_2 overnight.

Islet Perifusion Secretory Assay—Batches of ∼50 virally transduced islets placed in perifusion chambers were perifused with a KRB buffer containing 10 mM HEPES (KRBH; pH 7.4) and 0.07% bovine serum albumin at a flow rate of ∼1 ml/min at 37 °C. They were stimulated during a 10-min period with 2.8 mM glucose followed by a 40-min period with 16.7 mM glucose. Fractions were collected for insulin determination using a radioimmunoassay kit (Linco Research). At the end of each perifusion, islets were collected from the chamber and pelleted by centrifugation and lysed in acid-ethanol (0.2 mM HCl in 75% ethanol) for assessment of insulin content. Results are presented as insulin secreted normalized to islet insulin content.

RESULTS

RalA has previously been shown to be expressed in neuroendocrine cells (15). Immunoblotting demonstrated RalA was abundantly expressed in mouse pancreatic islets as well as two
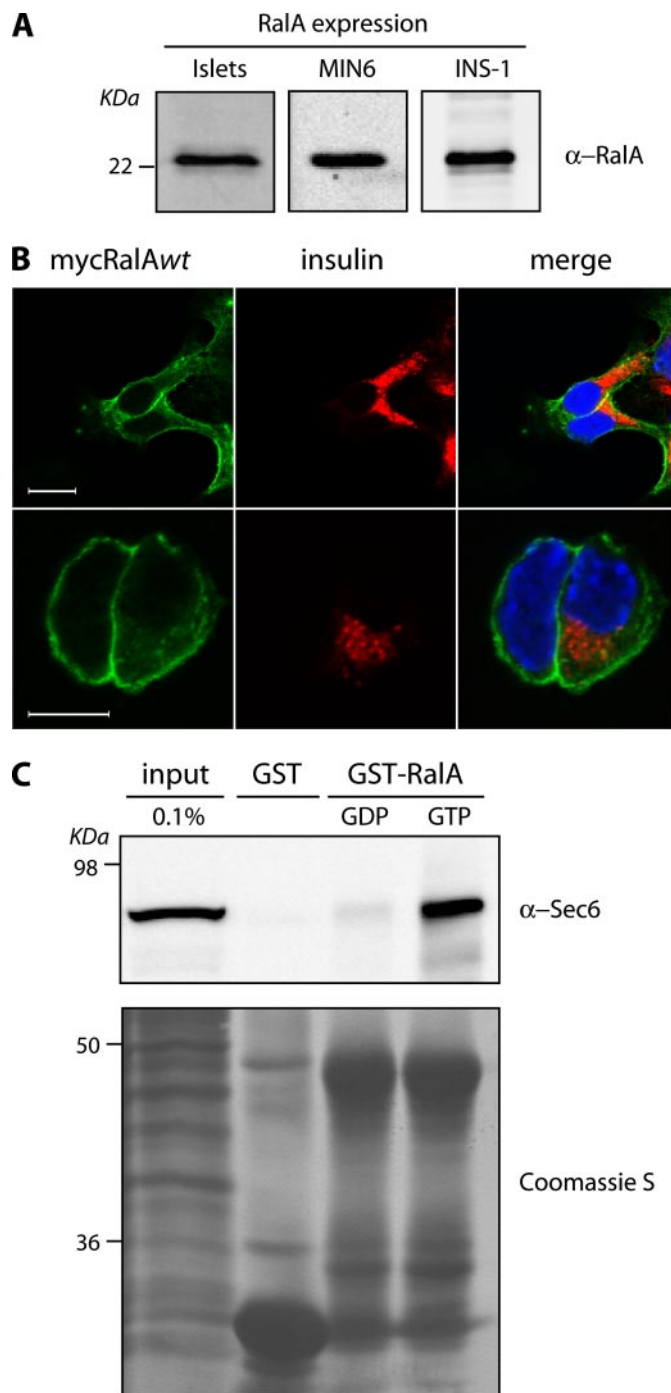

FIGURE 1. **RalA is expressed in insulin-secreting cells and localizes independently of insulin granules.** *A*, RalA is expressed in mouse pancreatic islets, mouse MIN6, and rat INS-1 insulin-secreting cell lines. Islet or whole cell lysates (6 μg) were immunoblotted for RalA. *B*, representative confocal images of adenoviral overexpressed Myc-epitope tagged RalA*wt* in MIN6 cells. RalA localizes independently of intracellular insulin granules. MIN6 cells were transduced with the RalA adenovirus at multiplicity of infection of 50. After 48 h, cells were fixed and labeled for RalA and insulin. RalA is shown in *green*, insulin is shown in *red*, and nuclei are shown in *blue* (4′,6-diamidino-2-phenylindole). All *scale bars* represent 10 μm. *C*, MIN6 total cell lysate was incubated for 1 h at 4 °C with GST control, GDP, or GTPγS nucleotide-loaded GST-RalA bound to glutathione-Sepharose beads. Shown is 0.1% of the starting material and $^{1}/_{2}$ the bound fraction immunoblotted for Sec6, and a Coomassie Blue stain (*Coomassie S*) of the membrane showing protein loading in these lanes. The blot is from a representative experiment (*n* = 3).

The Role of RalA in Insulin Secretion

insulin-secreting beta cell lines, mouse MIN6 and rat INS-1 cells (Fig. 1*A*), which suggests that RalA may be functionally important in the beta cell. Biochemical analysis in neurons demonstrated an abundance of Ral proteins in cholinergic synaptic vesicle fractions (16). One possibility is that RalA localizes to vesicles/granules to initiate tethering/docking steps at the plasma membrane, through association with the exocyst complex. We therefore examined the intracellular localization of RalA using immunofluorescence and confocal microscopy. MIN6 cells transduced with mycRalA*wt* adenovirus were labeled for RalA (anti-Myc) and insulin granules (anti-insulin). MycRalA was strongly expressed on the plasma membrane but also showed some intracellular labeling (Fig. 1*B*). However, intracellular RalA labeling appeared to be quite cytosolic and distinct from insulin granules, and thus RalA is unlikely to reside on these granules. We hypothesized that the Ral-exocyst interaction facilitates the tethering/docking of insulin granules at the plasma membrane. Hence we next set out to determine whether Ral interacts with the exocyst complex in MIN6 insulin-secreting cells. As shown in Fig. 1*C*, we observed a robust interaction between Sec6, a major exocyst subunit, and GTP-loaded RalA. However, there was only a weak interaction between GDP Loaded Ral and Sec6.

To examine the function of endogenous RalA on biphasic insulin secretion, we utilized an shRNA lentiviral delivery system for expression of control (Htr-1) or RalA shRNAs in mouse pancreatic islets. We then examined the biphasic insulin secretory response to glucose using the islet perifusion assay. RalA protein levels in mouse islets transduced with RalA shRNA (RalA KD) lentivirus were knocked down by 55% when compared with those of control islets transduced with Htr-1 shRNA (control) lentivirus (Fig. 2*A*). Basal insulin secretion in response to low glucose was markedly lower in RalA KD islets when compared with control islets (Fig. 2*B*), suggesting an important role for RalA in non-evoked constitutive exocytosis of insulin granules. The biphasic secretory pattern in response to high glucose (16.7 mM) was disrupted in RalA KD islets, in which the first phase characteristic transient burst of insulin release was markedly blunted, and subsequent sustained second phase insulin release was also severely reduced (Fig. 2*B*). This culminated in a significant ($p < 0.05$) 67% reduction in the overall glucose-stimulated insulin secretion (over basal secretion at low glucose) over the course of high glucose stimulation as analyzed by area under the curve analysis (10.79 ± 2.40 *versus* 3.60 ± 0.65) (Fig. 2*C*).

It has been postulated that the exocytosis of the RRP of insulin granules and mobilization of the reserve pool correspond to the first and second phases of insulin secretion, respectively (8). To examine the function of endogenous RalA on these insulin granule pools and their exocytotic kinetics, we further employed the shRNA lentiviral technique to deplete endogenous RalA protein in the rat INS-1 832/13 insulinoma cell line. We chose INS-1 832/13 as this cell line is excellent for performing patch clamp capacitance recording of insulin granule pool kinetics; however, INS-1 cells are notoriously difficult to transfect. We therefore first transduced INS-1 832/13 cells with control or RalA shRNA-expressing lentiviruses, and stable cell lines were then created by selection of GFP-positive cells.
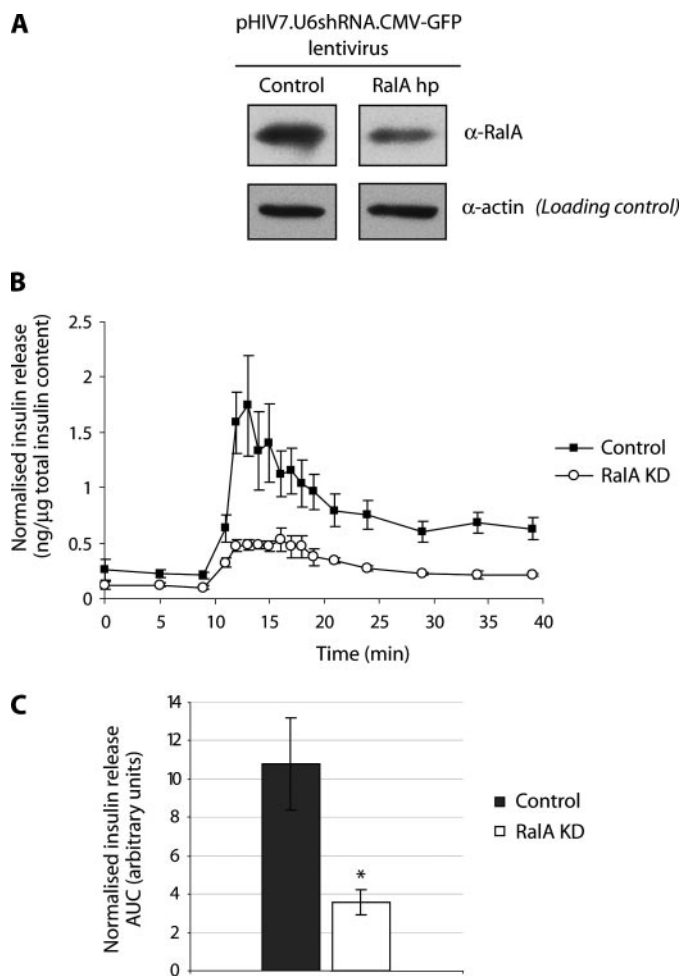

FIGURE 2. **RalA regulates insulin release from islets.** *A*, mouse islets were transduced with RalAshRNA or control shRNA lentivirus. Islet protein lysates (30 μg) were immunoblotted for RalA or actin. *B*, batches of 50 mouse islets were perifused with glucose as indicated. The insulin released was normalized to total insulin content ($n = 4–6$). *C*, means ± S.E. of area under the curves (*AUC*) of normalized insulin release from islet perfusions in *B*. Data represent insulin release from 11–30 min minus basal secretion (0–9 min). The *asterisk* indicates a statistically significant ($p < 0.05$) difference of the RalA KD when compared with control cells.

RalA shRNA-expressing cells demonstrated 40–50% less endogenous RalA protein when compared with control cells (Fig. 3*A*). We then performed patch clamp Cm measurements using the control shRNA- and RalA shRNA-expressing INS-1 832/13 cells. Insulin exocytosis was elicited by a protocol consisting of a train of eight 500-ms depolarization pulses. Cell Cm changes elicited by the first two pulses would approximate the size of the RRP of primed and fusion-ready granules. Subsequent pulses would estimate the rate of granule refilling or mobilization from the reserve pool(s) to the RRP, where the granules are subsequently primed for fusion competence (17). To reiterate, the size of the RRP and the rate of granule mobilization correlate with first and second phases of insulin secretion from whole pancreatic islets (18). Fig. 3*B* shows representative recordings of capacitance from control shRNA (*Control*) and RalA shRNA (RalA KD)-expressing cells. When compared with control cells, the Cm increase in RalA KD cells was significantly inhibited at every depolarizing pulse (Fig. 3*C*). Fig. 3*D* shows that the size of the
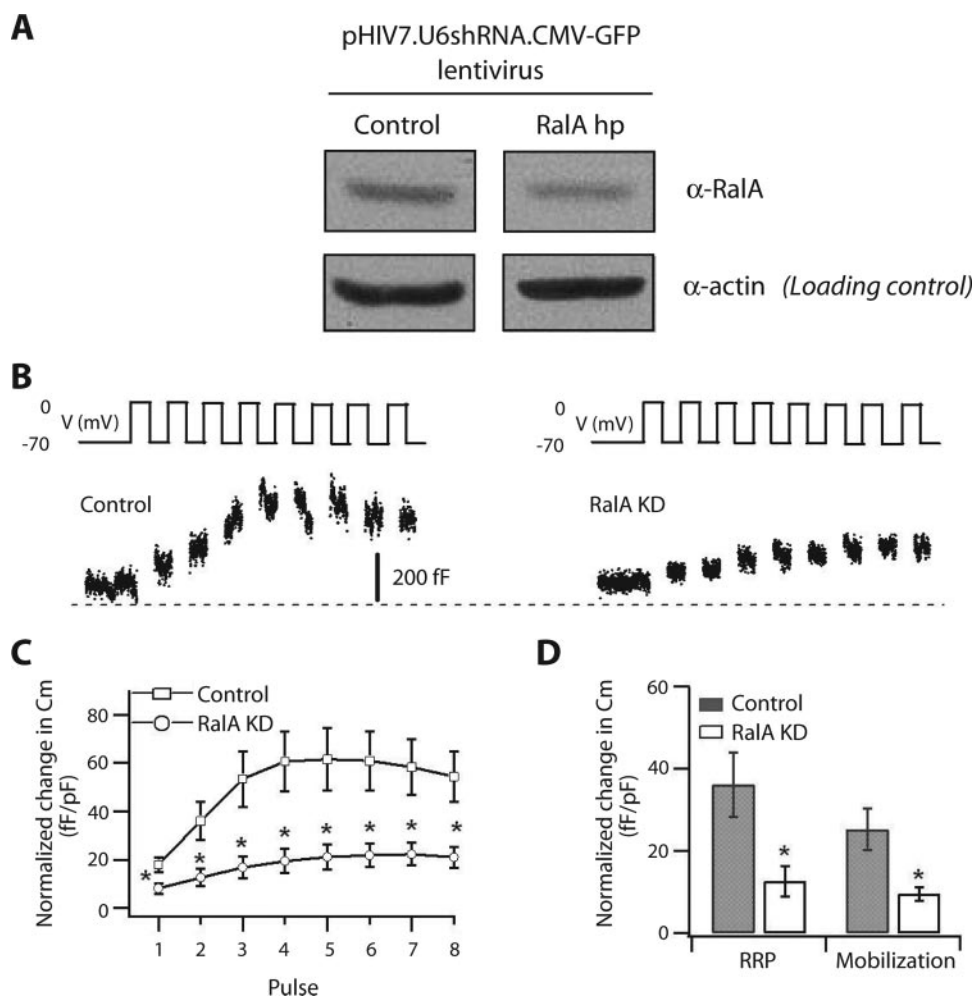
A

pHIV7.U6shRNA.CMV-GFP
lentivirus

B

C

D

FIGURE 3. RalA regulates insulin granule exocytosis. Changes in cell membrane capacitance (ΔCm) were measured from single INS-1 cells using a train of eight depolarizing pulses (500 ms in duration) from -70 mV to 0 mV. *A*, the RalA shRNA INS-1 cells show 40–50% less endogenous RalA protein when compared with the control cells. *B*, representative recordings of capacitance from Htr-1 shRNA (*Control*) and RalA shRNA (RalA KD) INS-1 cells. *C*, summary of the change in capacitance (ΔCm) normalized to basal cell membrane capacitance (fF/pF) from control ($n = 10$ cells) and RalA KD ($n = 9$ cells) INS-1 cells. Values represent the mean ± S.E. *D*, summary of the size of the RRP of insulin granules ($\Delta Cm_{1st-2nd\ pulse}$) and the rate of granule mobilization ($\Delta Cm_{3rd-8th\ pulse}$) ($n = 9–10$ cells). Values represent the mean ± S.E. *Asterisks* indicate a statistically significant ($p < 0.05$) difference of the RalA KD when compared with control cells.

RRP of granules ($\Delta Cm_{1st-2nd\ pulse}$) was significantly reduced by 65% ($p < 0.05$) in RalA KD cells (12.7 ± 3.6 fF/pF) when compared with control cells (36.1 ± 7.8 fF/pF). In addition, the rate of granule refilling/mobilization ($\Delta Cm_{3rd-8th\ pulse}$) was significantly reduced by 64% ($p < 0.05$) in RalA KD cells (22.3 ± 4.6 fF/pF) when compared with control cells (61.5 ± 12.8 fF/pF) (Fig. 3*D*). These results suggest that RalA knockdown greatly impairs depolarization-induced exocytosis by affecting release of the RRP of granules and mobilization of granules from reserve pool(s).

We then began to explore the cell signaling by which secretagogue stimulation is coupled to RalA-mediated insulin secretion. As RalA is a GTPase, we examined the functional domains within RalA that are regulated by guanine nucleotides and whether such nucleotide regulation is required for secretagogue-stimulated insulin secretion. We constructed adenoviruses with Myc-epitope tagged RalA*wt*, RalAG23V (GTP-active), and RalAS28N (GDP-inactive). Adenoviral transductions

in MIN6 cells resulted in ~100% transduction efficiencies (Fig. 4*B*) and significant overexpression for each of the three exogenous RalA proteins (Fig. 4*C*). To assess the role of RalA on insulin secretion, MIN6 cells were transduced with empty virus, RalA*wt*, RalAG23V, and RalAS28N virus, and insulin secretion was induced by KCl or combinations of glucose and carbachol or glucose and KCl and measured using insulin radioimmunoassays. Fig. 4*A* shows the effect of RalA overexpression on secretagogue-stimulated insulin secretion. Overexpression of RalA*wt* significantly ($p < 0.05$) potentiated insulin secretion across all secretagogue stimuli when compared with the empty virus control. The RalAG23V mutant significantly ($p < 0.05$) potentiated glucose/KCl-induced insulin secretion when compared with the empty virus control. However, the RalAG23V mutant did not significantly affect KCl or glucose/carbachol-induced insulin secretion despite the tendency for a potentiation. The RalAS28N mutant significantly inhibited ($p < 0.05$) KCl-induced insulin secretion but had no significant effect on glucose/carbachol- and glucose/KCl-induced insulin secretion despite an inhibitory trend. It is apparent that the nucleotide state of RalA affects the level of insulin secreted from these cells under these conditions since cells expressing the RalA mutant with higher affinity for GTP (RalAG23V) displayed elevated insulin secretion when compared with cells expressing the RalA mutant with a higher affinity for GDP (RalAS28N). These data demonstrate that the action(s) of RalA in regulating insulin secretion is at least in part by acting as a substrate for guanine nucleotides.

DISCUSSION

In this study, RalA has been demonstrated to be an active component of regulated insulin secretion in pancreatic beta cells. RalA RNA interference-mediated knockdown of endogenous RalA protein expression in mouse pancreatic islets dramatically inhibited biphasic insulin release. Furthermore, patch clamp Cm experiments of RalA INS-1 832/13 cells showed that the inhibition of insulin secretion is directly attributed to the reduction in the exocytosis of the RRP of granules. RalA was found to interact with the endogenous exocyst complex in a nucleotide-dependent manner, and consistent with this inter-
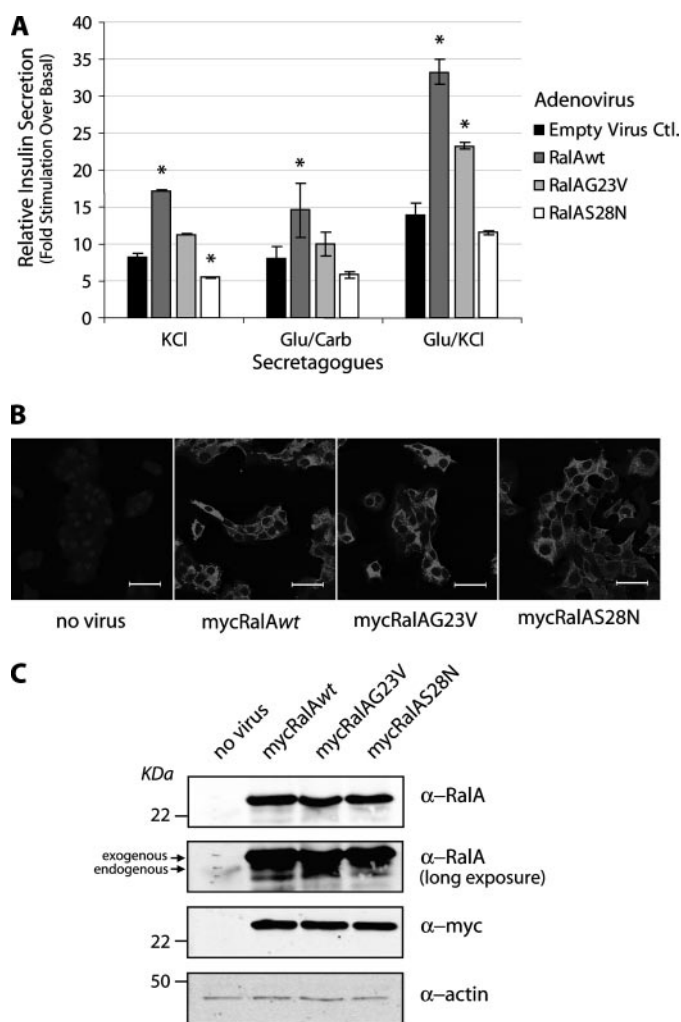
FIGURE 4. RalA overexpression regulates secretagogue-stimulated insulin release from MIN6 beta cells. *A,* MIN6 cells were transduced with empty virus, mycRalAwt, mycRalAG23V, and mycRalAS28N and grown in low glucose medium (6 mM glucose) for 48 h before stimulating the cells with various secretagogues. Cells were either unstimulated or stimulated with KCl (30 mM), glucose/carbachol (25 mM/100 μM), or glucose/KCl (25 mM/30 mM) for 1 h. Insulin secretion was measured using insulin radioimmunoassays of samples from the cell supernatants. Data shown are from two independent experiments assayed in duplicate. Insulin secretions are expressed as -fold over basal secretion for each virus. *Asterisks* indicate a statistically significant ($p <$ 0.05) difference from the empty virus control (*Empty Virus Ctl.*); MIN6 cells were transduced with Myc-epitope tagged RalAwt, RalAG23V, and RalAS28N recombinant adenovirus. Cells were fixed, labeled for RalA (Myc), and examined by confocal microscopy (*B*). *Scale bars* represent 30 μm, or cells were lysed and immunoblotted for RalA and actin (*C*).

action, adenoviral overexpression of guanine nucleotide-binding mutants of RalA demonstrated that RalA acts in a nucleotide-dependent manner to influence secretagogue-stimulated insulin secretion. The localization of RalA appeared to be independent of insulin granules but abundant on the plasma membrane. We propose that RalA is a positive regulator of insulin granule exocytosis, which acts at the plasma membrane together with the exocyst complex to facilitate the replenishment of the RRP of insulin granules.

The steps involving the tethering, docking, priming, and fusion of insulin granules have not yet been clearly delineated. The least understood of this very complex exocytotic process is that of granule tethering and docking that we propose is regulated by the exocyst complex and RalA and which precedes granule priming. The mammalian exocyst complex has recently been implicated in insulin secretion (10), and the authors suggest that Sec6 may be delivered to the cell surface on insulin granules and facilitate tethering/docking by interactions with other exocyst subunits including Sec8 at the plasma membrane. In the present study, we found that RalA localizes to both the plasma membrane and the cytosol, but we were unable to identify any significant labeling of secretory granules. Hence, we propose that RalA most likely acts at the plasma membrane to regulate the exocyst and facilitate tethering and docking directly and that this association occurs independent of the granules. In the present study, RalA was shown to interact with the exocyst complex in a GTP-dependent manner, consistent with previous studies (11), and this is thought to regulate exocyst complex assembly (5). Furthermore, we found that adenoviral overexpression of nucleotide-preferential RalA mutants had differential effects on insulin secretion. Under some conditions, the GTP-bound RalAG23V mutant potentiated insulin secretion and the RalAS28N mutant inhibited insulin secretion. These results suggest that RalA binding to the exocyst is required for the efficient exocytosis of insulin granules. Of interest is the fact that the *wt* RalA was found to potentiate insulin secretion under all conditions. The exogenous *wt* RalA would likely undergo cycling between GDP- and GTP-bound forms similar to the endogenous protein, and this capacity for repeated cycling of *wt* RalA could explain its greater efficiency than GTP-bound RalAG23V in potentiating insulin secretion. This suggests that it is not simply the ability of RalA to bind the exocyst that is the rate-limiting step in this process but also the ability of RalA to execute this step following GTP hydrolysis.

In the present study, we demonstrated using glucose perifusion experiments that mouse islets with depleted RalA displayed dramatic inhibition in both the first and the second phases of insulin secretion. Consistent with these findings, patch clamp Cm in RalA knockdown cells inhibited both the initial exocytic events correlating with the fusion of the RRP of granules and subsequent exocytic events, which correlates with the mobilization and exocytosis of the reserve pool of granules. We propose that RalA acts at the granule-tethering step, which would precede the granule-priming and fusion steps, and hence, profoundly influence the RRP and granule mobilization of insulin granules that underlie the initial and late phases of insulin secretion. This is supported by the findings of Polzin *et al.* (19), who generated transgenic mice expressing the RalAS28N mutant. Synaptosomes isolated from RalAS28N transgenic mice showed impairments in the replenishment of the RRP of vesicles when compared with *wt* synaptosomes. Moreover, Tsuboi *et al.* (10) suggest that disruption of the exocyst complex in beta cells results in a perturbation of granule supply to docking sites and consequently fewer docking events. Importantly, they also observed defects in KCl-induced insulin secretion, which may be due to a reduced RRP.

A study by Ohara-Imaizumi *et al.* (20) examined the kinetics of insulin granule docking in response to secretagogues using real-time total internal reflection fluorescence microscopy and found that the first phase of insulin secretion strongly correlated with KCl-induced fusion of predocked insulin granules. In

addition, the first and second phases of insulin secretion induced by glucose stimulation correlated with the fusion of predocked and newly recruited granules. This is an ideal technique for examining the spatio-temporal behavior in insulin granule docking and fusion events and would greatly benefit future studies aimed at elucidating the precise molecular role of RalA in insulin granule docking and secretion.

REFERENCES

1. Chardin, P., and Tavitian, A. (1986) *EMBO J.* **5,** 2203–2208
2. Shen, Y. J., Xu, L. Z., and Foster, D. A. (2001) *Mol. Cell. Biol.* **21,** 595–602
3. Ohta, Y., Suzuki, N., Nakamura, S., Hartwig, J. H., and Stossel, T. P. (1999) *Proc. Natl. Acad. Sci. U. S. A.* **96,** 2122–2128
4. Hamad, N. M., Elconin, J. H., Karnoub, A. E., Bai, W. L., Rich, J. N., Abraham, R. T., Der, C. J., and Counter, C. M. (2002) *Gene Dev.* **16,** 2045–2057
5. Moskalenko, S., Henry, D. O., Rosse, C., Mirey, G., Camonis, J. H., and White, M. A. (2002) *Nat. Cell Biol.* **4,** 66–72
6. Wang, L., Li, G., and Sugita, S. (2004) *J. Biol. Chem.* **279,** 19875–19881
7. Henquin, J. C. (2000) *Diabetes* **49,** 1751–1760
8. Barg, S., Eliasson, L., Renstrom, E., and Rorsman, P. (2002) *Diabetes* **51,** S74–S82
9. Jin, R. S., Junutula, J. R., Matern, H. T., Ervin, K. E., Scheller, R. H., and Brunger, A. T. (2005) *EMBO J.* **24,** 2064–2074
10. Tsuboi, T., Ravier, M. A., Xie, H., Ewart, M. A., Gould, G. W., Baldwin, S. A., and Rutter, G. A. (2005) *J. Biol. Chem.* **280,** 25565–25570
11. Brymora, A., Valova, V. A., Larsen, M. R., Roufogalis, B. D., and Robinson, P. J. (2001) *J. Biol. Chem.* **276,** 29792–29797
12. Li, M. J., and Rossi, J. J. (2005) *Methods Enzymol.* **392,** 218–226
13. Lindau, M., and Neher, E. (1988) *Pfluegers Arch. Eur. J. Physiol.* **411,** 137–146
14. Kwan, E. P., Xie, L., Sheu, L., Ohtsuka, T., and Gaisano, H. Y. (2007) *Diabetes* **56,** 2579–2588
15. Vitale, N., Mawet, J., Camonis, J., Regazzi, R., Bader, M. F., and Chasserot-Golaz, S. (2005) *J. Biol. Chem.* **280,** 29921–29928
16. Volknandt, W., Pevsner, J., Elferink, L. A., and Scheller, R. H. (1993) *FEBS Lett.* **317,** 53–56
17. Gillis, K. D., Mossner, R., and Neher, E. (1996) *Neuron* **16,** 1209–1220
18. Rorsman, P., and Renstrom, E. (2003) *Diabetologia* **46,** 1029–1045
19. Polzin, A., Shipitsin, M., Goi, T., Feig, L. A., and Turner, T. J. (2002) *Mol. Cell Biol.* **22,** 1714–1722
20. Ohara-Imaizumi, M., Nakamichi, Y., Tanaka, T., Ishida, H., and Nagamatsu, S. (2002) *J. Biol. Chem.* **277,** 3805–3808

The Journal of Biological Chemistry